Earth Syst. Sci. Data, 15, 607–616, 2023
https://doi.org/10.5194/essd-15-607-2023

Open Access Earth System Science Data

Annual hydrographic variability in Antarctic coastal waters infused with glacial inflow

Maria Osińska[1], Kornelia A. Wójcik-Długoborska[2], and Robert J. Bialik[2]

[1]Institute of Oceanography, University of Gdańsk, Piłsudskiego 46, 81-378 Gdynia, Poland
[2]Institute of Biochemistry and Biophysics, Polish Academy of Sciences,
Pawińskiego 5a, 02-106 Warsaw, Poland

Correspondence: Robert J. Bialik (rbialik@ibb.waw.pl)

Received: 16 September 2022 – Discussion started: 4 October 2022
Revised: 14 December 2022 – Accepted: 10 January 2023 – Published: 7 February 2023

Abstract. During the 38 months between December 2018 and January 2022, multiparameter hydrographic measurements were taken at 31 sites within Admiralty Bay, King George Island, Antarctica. These records consisted of water column measurements (down to 100 m) of temperature, conductivity, turbidity, and pH as well as the dissolved oxygen, dissolved organic matter, chlorophyll-*a* and phycoerythrin contents. The sites were chosen due to their variable distances from glacial fronts and open ocean waters. Fifteen sites were localized within smaller glacial coves, with waters highly impacted by glacial infusions; seven sites were located in the open waters of the main body of Admiralty Bay; and nine sites were located in the intermediate conditions of the Ezcurra Inlet. The final dataset consists of measurements carried out over 142 separate days, with an average of 3.74 measurements per month. However, data were not collected regularly throughout the year and were collected less frequently during winter, although data were gathered for all but 2 winter months. On average, each site was investigated 98.2 times. Due to calibration issues, absolute values of optically measured properties occasionally show unrealistic negative values, but the relative distributions of these values remain valid. Variabilities in the measured properties each season and throughout the whole duration of the project reveal regular oscillations as well as possible long-term trends. The described dataset is freely available at PANGAEA: https://doi.org/10.1594/PANGAEA.947909 (Osińska et al., 2022).

1 Introduction

When freshwater from glaciers is introduced to marine environments, it mixes with ambient ocean water masses, leading to the formation of new glacially modified water (GMW; Straneo, 2012). In this way, freshwater export has been shown to influence properties of the coastal ocean, with impacts on the hydrodynamics and thermodynamics (Bendtsen et al., 2015; Chauché et al., 2014). Therefore, there are significant justifications to investigate water quality properties in glacial bays and fjords and to track their variability in order to potentially predict future changes.

While the majority of studies examining the influence of glacial meltwater on the marine ecosystem have been performed in the Northern Hemisphere, the importance of the effect of glacial meltwater for the functioning of coastal Antarctic waters has long been hypothesized. Nevertheless, widely available data that describe water quality in glacial bays beyond seasonal timescales at high sampling resolutions and that examine multiple variables remain nonexistent. In fact, such datasets are scarce for the Arctic and Alaska as well.

To address this deficiency, an intricate investigation campaign was designed with the intention of comprehensively observing the seasonal oscillations and long-term trends in water quality variability in Admiralty Bay (AB), King George Island, Western Antarctica. The goal of this project was to widen the scope of previously gathered observations by expanding the overall duration of monitoring, increasing

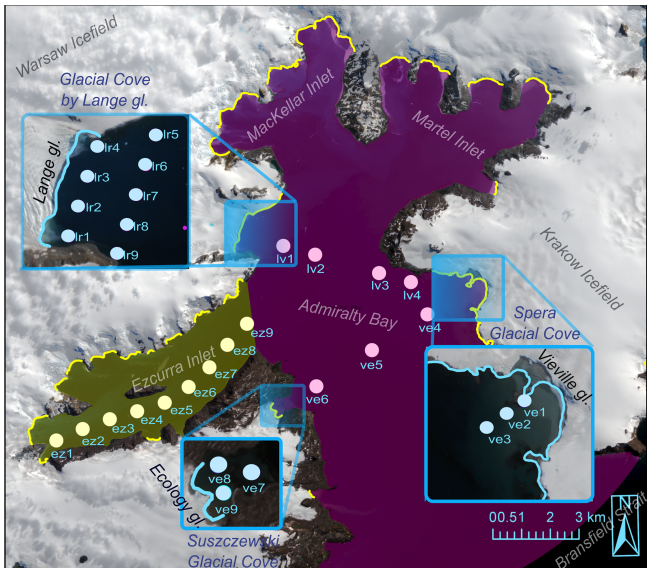

Figure 1. Map of Admiralty Bay showing the measurement points in the following three distinct zones: the main body of Admiralty Bay (pink), glacial coves (blue inset boxes) and the Ezcurra Inlet (yellow lines based upon Gerrish et al., 2021). Bright yellow denotes the current position of the ice–water coastline, and the bright blue insets show the position of the coastline on 10 March 2018. (Sourced from Sentinel imagery, 29 December 2021.)

the frequency and number of measured parameters, and to acquire data across all seasons of the year.

2 Research area

AB is a 177.04 km^2 cove southeast of King George Island, the largest island of the South Shetland Islands in Western Antarctica. In its interior, AB is subdivided into three distinct areas: the Ezcurra, Mackellar and Martel inlets, which all blend together approximately 11 km from the open ocean waters of the Bransfield Strait, forming the main body of AB (Fig. 1). Its coastline has a length of 150 km: 102 km consists of rocky coastline, and the remaining 38 km consists of ice–water boundaries (Fig. 1, yellow lines; Gerrish et al., 2021). The tidewater glaciers that form these frontiers are the outer regions of two large icefields, the Warsaw and Kraków icefields. Both icefields are reportedly experiencing unprecedented transformation due to the effects of climate warming (Rückamp et al., 2010; Dziembowski and Bialik, 2022) and are draining into AB through numerous glacial creeks.

The dataset as a whole was split into three different zones within the AB, identified based on distinct seawater properties and proximity to both glacial fronts and the mouth of the bay (i.e. proximity to open ocean source waters). These include the following:

- *Glacial coves*, comprising distinct smaller bays formed near tidewater glaciers in which marine waters are under the direct influence of glacial meltwater input. Here, three glacial coves were analysed in depth, namely the cove near Lange Glacier (1.50 km^2 in area with a 2.81 km long ice–water frontline), Spera Cove (2.45 km^2 in area with a 4.33 km long ice–water frontline) near Vieville (Viéville) Glacier and Suszczewski Cove near Ecology Glacier (0.69 km^2 in area with a 0.36 km long ice–water frontline). All three of these basins are undergoing long-term transformation caused by continuously moving and developing glacial fronts. This is visualized in Fig. 1, where the light blue line on the glacial cove insets represents the ice–water boundary in 2018 (based on a Sentinel satellite image from 10 March 2018), which is different from the frontline shown in the satellite picture presented in Fig. 1 taken in December of 2021 (Sentinel, 29 December 2021). The change is especially noticeable in Spera Cove near Vieville Glacier, where the ice front has retreated 500 m within 3 years in some locations.

- *The main body of Admiralty Bay*, comprising open bay waters in the main body of the cove, most directly influenced by the open ocean waters of the Bransfield Strait with which it is connected by a 13.45 km wide outlet. Nevertheless, this location is also affected by glacial input, especially in its northern parts.

- *Ezcurra Inlet*, comprising an intermediate area (of 21.32 km^2) separated from Admiralty Bay waters by a relatively narrow passage (2.40 km wide) and influenced by the surrounding ice coastline (9.58 km of the 32.67 km long coastline).

These areas are shown in Fig. 1 and are used as separate, although deeply interrelated, regions for further study. To that end, measurement points were chosen, and their locations are marked on the map in Fig. 1; their details (location, depth, number of measurements performed at a given point, and, in the case of glacial cove points, distance from the water–ice boundary) are summarized in Table 1.

Measurements in the glacial coves and Admiralty Bay were taken from December 2018 until January 2022, whereas measurements in Ezcurra Inlet took place from October 2019 until January 2022.

Due to the proximity to glaciers and the harsh Antarctic weather, sampling in this region was especially strenuous. Each measurement campaign lasted only a few hours and was performed from the decks of small Zodiac boats (Fig. 2) that provided little comfort to the crew. Moreover, getting to the assigned sites often involved manoeuvring through moving ice packs and bits of icebergs coming from calving glaciers. Sampling during the winter months required working in the dark, in extremely cold temperatures and with continuous contact to freezing water.

Table 1. Details of the measurement sites. The depth measurements are based on the YSI EXO sonde depth sensor; depths > 100 at a given site indicate that the sonde was lowered to the cable limits (100 m) and did not reach the ocean bottom. Distances from glacial fronts were measured only for sites within smaller glacial coves adjacent to individual glaciers, as sites in Admiralty Bay and Ezcurra Inlet were influenced by a number of glaciers in their vicinity.

Site name and zone	Latitude	Longitude	Depth (m)	Distance from glacial front (m) (2018–2021)
Glacial coves				
lr1	−62.1227	−58.4892	19	315–322
lr2	−62.1195	−58.4868	> 100	266−330
lr3	−62.1163	−58.4845	> 100	275–332
lr4	−62.1131	−58.4821	23	260–343
lr5	−62.1120	−58.4687	8	940–1018
lr6	−62.1152	−58.4711	66	880–951
lr7	−62.1184	−58.4734	> 100	902–952
lr8	−62.1216	−58.4758	> 100	868–912
lr9	−62.1247	−58.4782	3	929–932
ve1	−62.1361	−58.3380	2	71–481
ve2	−62.1375	−58.3429	8	359–780
ve3	−62.1391	−58.3483	29	686–1118
ve7	−62.1716	−58.4613	4	455–469
ve8	−62.1709	−58.4677	2	210–232
ve9	−62.1734	−58.4668	3	113–128
Admiralty Bay				
lv1	−62.1221	−58.4624	> 100	
lv2	−62.1251	−58.4412	> 100	
lv3	−62.1313	−58.3989	71	
lv4	−62.1343	−58.3777	17	
ve4	−62.1445	−58.3671	58	
ve5	−62.1553	−58.4047	> 100	
ve6	−62.1662	−58.4424	55	
Ezcurra Inlet				
ez1	−62.1812	−58.6172	56	
ez2	−62.1778	−58.5994	67	
ez3	−62.1750	−58.5811	51	
ez4	−62.1727	−58.5626	61	
ez5	−62.1702	−58.5441	68	
ez6	−62.1655	−58.5279	84	
ez7	−62.1595	−58.5136	> 100	
ez8	−62.1526	−58.5012	> 100	
ez9	−62.1462	−58.4878	> 100	

3 Methodology

3.1 Measured water properties

Measurements were performed with two professional YSI multiparameter EXO sondes (EXO1 and EXO2); these instruments have been designed for simultaneous investigation of multiple water quality properties and have also been used and tested by researchers worldwide (Snazelle, 2015). EXO1 consists of five sensor ports, and EXO2 contains seven ports; therefore, the water properties measured varied between the particular campaigns. Of the 3045 measurements collected, 2069 were acquired using the EXO1 sonde, and the remaining 976 were acquired with EXO2 and its larger sensor capacity (details seen in Fig. 2).

The list of the sensors and the properties investigated by each are summarized in Table 2. Some hydrographic properties are derived from direct sensor measurements (e.g. turbidity from light scatter). In these cases, the sondes automatically calculated the additional related values based on universally accepted formulas (Table 2).

Table 2. List of sensors and measured water properties (based upon YSI Inc, 2017).

		Sensor	Measured property	Unit	Accuracy/linearity	Direct measurement (D) or calculated from other measurement (C)
EXO2	EXO1	Conductivity/ Temperature	Conductivity	µS cm^{-1}	0–100 mS cm^{-1}: ±0.5 % of reading or 0.001 mS cm^{-1}, whichever is greater; 100–200 mS cm^{-1}: ±1 % of reading	D
			Specific conductivity	µS cm^{-1}		C – conductivity adjusted to temperature
			nLF conductivity	µS cm^{-1}		C – with temperature compensation
			Salinity	PSU		C – based on temperature and conductivity using APHA (1989)
			Temperature	°C	±0.01°	D
		Depth and level	Pressure	PSI	±0.04 m	D
			Depth	m		C – based on water and atmospheric pressure
		Dissolved oxygen	Dissolved oxygen	mg L^{-1}	±1 % of reading or ±0.01 mg L^{-1}	C – using Stern–Volmer equation from luminescence measurement corrected with temperature and atmospheric pressure
			Dissolved oxygen saturation	%		
			Dissolved oxygen local saturation	%		
		pH	pH	–, mV	±0.01	C – from electric potential difference
		Turbidity	Turbidity	FNU	0.3 FNU or ±2 % of reading, whichever is greater	C – from light scatter
	Not measured by EXO1	fDOM	Dissolved organic matter	QSU, RFU	$R^2 > 0.999$ for serial dilution of 300 ppb quinine sulfate solution	C – from fluorescence
		Total algae (Chl and BGA)	Chlorophyll *a*	µg L^{-1}, RFU	$R^2 > 0.999$ for serial dilution of rhodamine WT solution from 0 to 400 µg L^{-1} Chl equivalents	C – from fluorescence
			BGA PE (phycoerythrin)	µg L^{-1}, RFU	$R^2 > 0.999$ for serial dilution of rhodamine WT solution from 0 to 280 µg L^{-1} PE equivalents	C – from fluorescence

The abbreviations used in the table are as follows: nLF – non-linear function, PSU – practical salinity units, fDOM – fluorescent dissolved organic matter, FNU – formazin nephelometric units, QSU – quinine sulfate units, RFU – relative fluorescence units, Chl – chlorophyll, BGA – blue-green algae and PE – phycoerythrin.

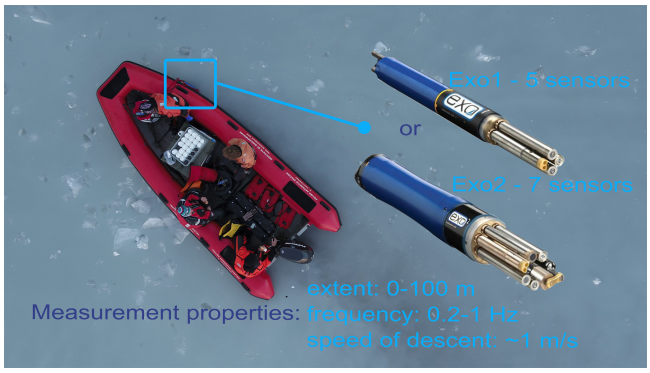

Figure 2. The images in the foreground (sourced from https://observator.com/products/ysi-exo-series-multiparameter-sonde/, last access: 3 September 2022) present the sondes used to make the measurements, and the text at the bottom of the panel outlines the measurement properties. The background image shows scientists in a Zodiac boat during measurements of water properties; the water is visibly infused with turbid GMW.

3.2 Measurement and data handling procedure: causes of possible data errors and missing values

Measurements were conducted from the deck of a Zodiac boat (Fig. 2). When the boat was at the designated point, the sonde was lowered by the cable from the reel to a maximum depth of 100 m. At sites with depth of less than 100 m (see Table 1 for information on sites' depths), the measurements were performed throughout the whole water column (until sea bottom was reached). At sites where the depth surpassed 100 m, data were only collected from the top 100 m; this is a limitation of this study, as data were not obtained from bottom portions of the water column. The sampling rate of the sondes was initially 0.2 Hz until 30 December 2019; after 30 December 2019, the sampling frequency increased to 1 Hz.

The intended descent rate of the instrument was $1\,m\,s^{-1}$; however, as this was manually controlled by the research personnel, the descent rate of the sonde varied significantly. Furthermore, the fact that the measurements were acquired by different crews may cause some discrepancy in the acquired data. The sensitivity of particular sensors varied. Therefore, if the probe was lowered too quickly, the measurements taken by some sondes may incorrectly correlate with the depth attributed to those measurements.

Other obstacles were caused by challenging weather and sea conditions. Waves and surface currents often considerably influenced the position of the boat, making it impossible to remain stationed at the assigned site location for the duration the cast. This can be seen from the position data recorded via handheld GPS during sensor deployment and included within the data file. Currents below the surface moved the sonde and cable horizontally from the initial cast position by an unknown extent.

On numerous occasions, ice prevented scientists from reaching specific sites. This was frequently the case in areas close to glacial fronts, most notably when the water surface froze during the winter months and when glacial calving increased in the summer.

All of the sensors were calibrated in accordance with guidelines found in the YSI EXO manual (YSI Inc, 2017), and they were replaced after the appropriate time or when malfunctions occurred that could not be otherwise resolved. The depth and level sensor was calibrated at the start of every survey day.

Measured data were initially recorded in the YSI proprietary format in software embedded into all of the sensors. At this stage, data went through real-time data filtering using a basic rolling filter as well as adaptive filtering and outlier rejection with the default manufacturer settings (for details, see YSI Inc, 2017). Gathered data were later downloaded using KorEXO software and exported to MATLAB where some outliers and extreme values were extracted due to one of the following reasons:

- notes from the measurement crew that indicated malfunctions or some other issues;
- the sonde showed unrealistic values from all of the sensors after reaching the bottom (caused by the contact with seafloor) at sites with depths of less than 100 m;
- the presence of other extreme values and outliers, which were scrutinized individually, such as continuous abnormal values from a particular sensor during a measurement day (indicating sensor malfunction or decalibration) or incidental extreme values recorded within otherwise reasonable datasets (indicating momentary disturbances).

Despite this series of steps, the whole dataset did not go through any formalized quality assessment/quality check procedure.

Optical sensors for total algae and fluorescent dissolved organic matter (fDOM) showed unrealistic negative values (77.82 % of chlorophyll *a*, 70.87 % of phycoerythrin and 60.45 % of fDOM readings). This was most probably caused by the chosen calibration method that employed a one-point procedure based on deionized water as a proxy for the zero fluorescence standard. This methodology was outlined by the sensor manufacturer (YSI Inc, 2017) but has proven insufficient in this environment; this suggests the necessity for a more robust method of calibration for future measurements. Nevertheless, these negative values have been retained in the data file because they represent the correct variability in the properties; however, their absolute values should be considered carefully, and more attention should be given to the relative units (RFU) for chlorophyll *a*, phycoerythrin and fDOM.

The turbidity sensor also showed negative values (19.56 % of the readings), but it was calibrated using a two-point procedure with an appropriate standard, and its FNU values

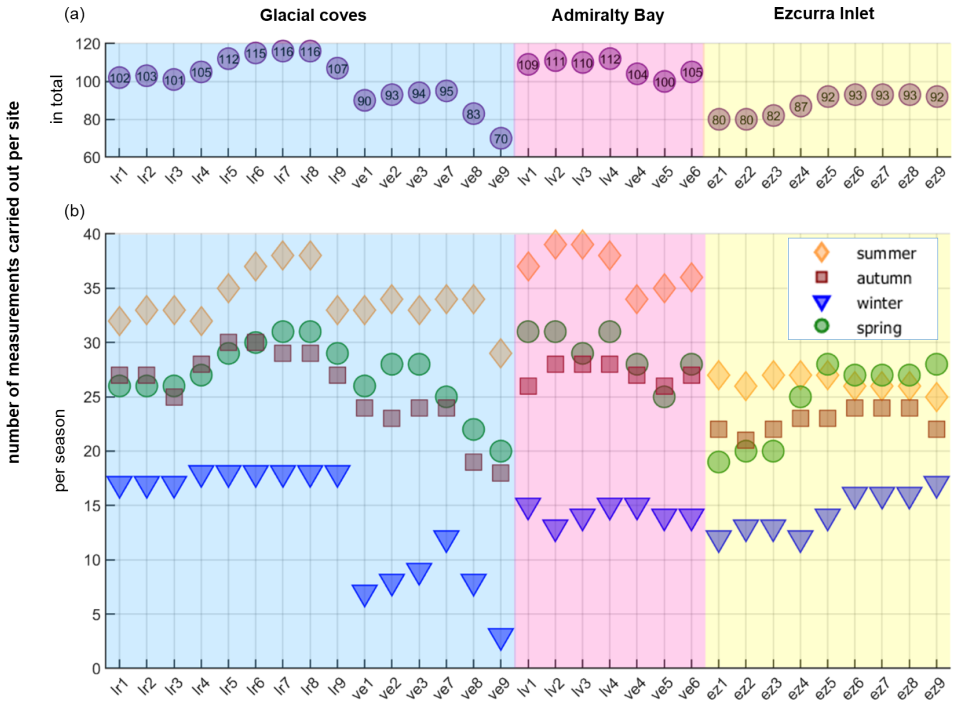

Figure 3. Number of measurements taken at the designated sites **(a)** in total and **(b)** by season (calendar) in the period from December 2018 to January 2022.

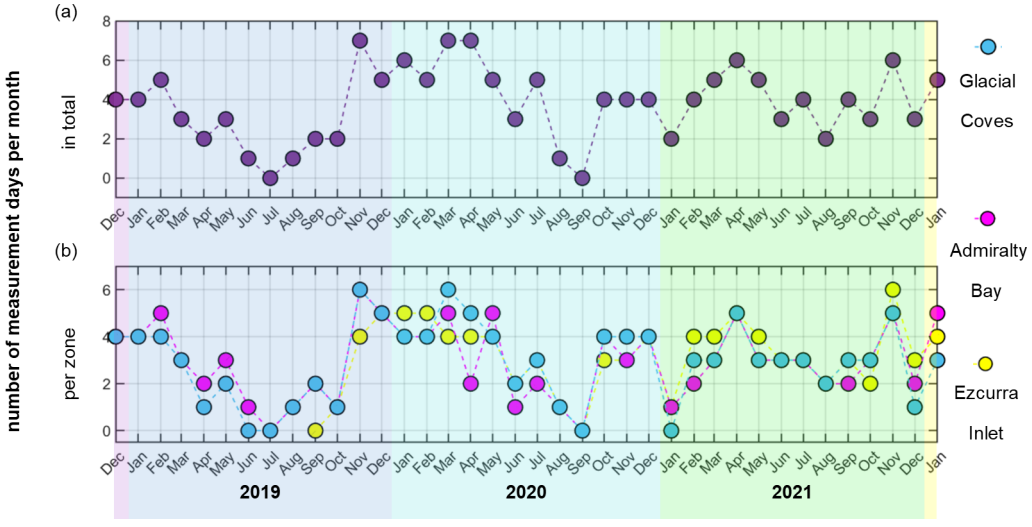

Figure 4. Number of measurement days per month **(a)** in total and **(b)** per zone (counted days on which measurements have been performed at at least half of zone's sites).

have been confirmed in Admiralty Bay waters via the laboratory procedure explained in detail by Wojcik-Długoborska et al. (2022).

4 Results

The results of the measurement campaign discussed above consist of a large and complex dataset describing the variability in the physical, chemical and biological properties in glacially influenced bays. Figure 3 presents a summary of the total number of investigations performed. This shows that, even at the sites sampled the least, it was possible to gather data during all seasons. However, most studies were performed during summer across all zones, while the fewest measurements were collected in winter. Interestingly, despite the unpredictable conditions in the glacial coves, the number

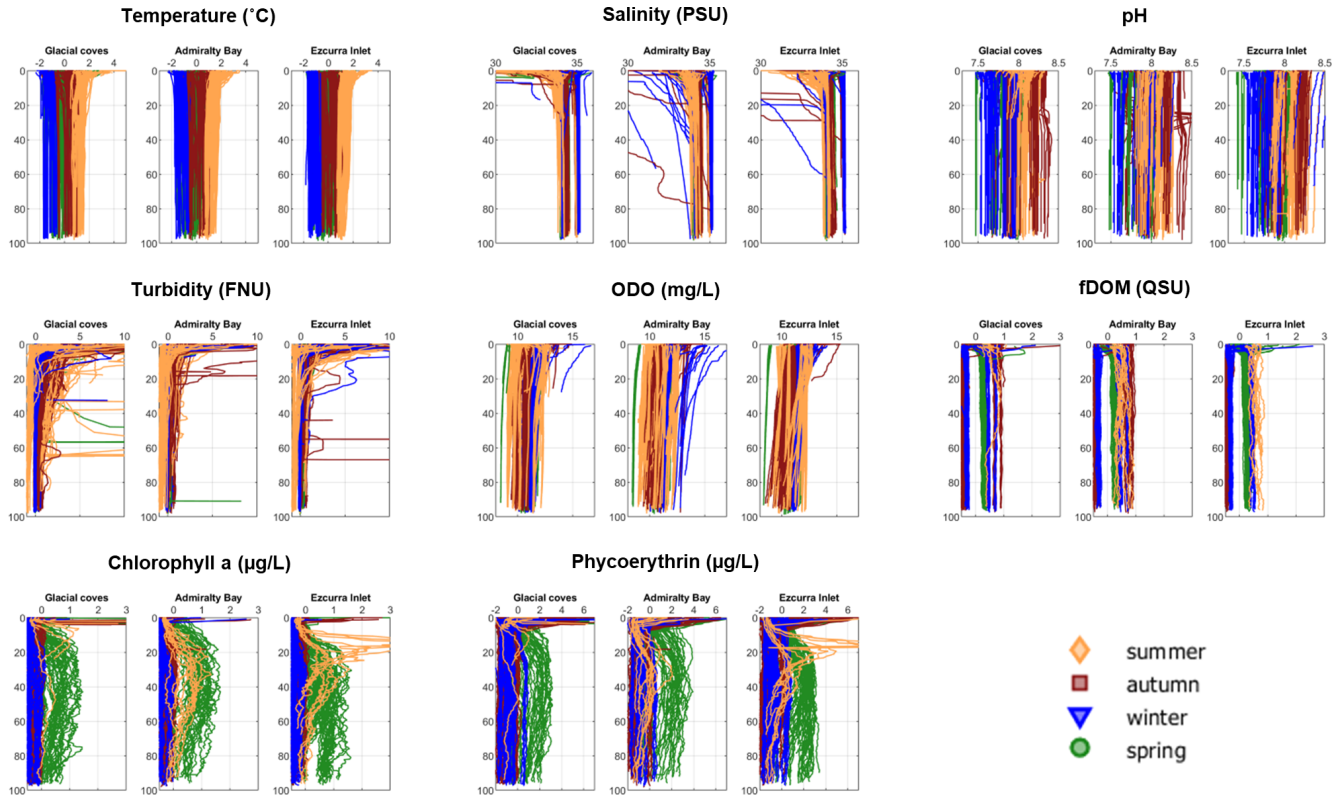

Figure 5. Vertical variability in measured properties divided by zone and season.

of surveys at each site fluctuates at around 100 per location (average of 98.2 measurements per site), which is promising for future statistical analysis.

Considering the complete duration of the projects (see Fig. 4), it is noticeable that the number of measurement days fluctuated, with increases during the warmer seasons when there was a maximum of 7 measurement days per month. In Fig. 4b, we observe that the same tendencies apply to all of the zones, and none of them have been more frequently investigated to any degree of significance. The average number of measurements per month was 3.74 in the glacial coves and 2.91 in Admiralty Bay, with the same number of successful measurement days (111) throughout the whole duration of the project, and 2.42 for Ezcurra Inlet over 92 measurement days.

The division of sites into three zones shows how proximity to glacial fronts and open ocean waters alters particular water quality properties. This effect is also notably correlated with seasonal shifts (Figs. 5, 6). In Fig. 5, the vertical distribution of all of the gathered data is presented. It is apparent that temperature, pH, optical dissolved oxygen (ODO), fDOM and phytoplankton pigment values are especially prone to change due to seasonal shifts, whereas salinity and turbidity values remain similar throughout the year. However, Fig. 6 provides a detailed illustration of how different properties vary in surface layers in contrast with the whole water column (limited to 100 m depth), most notably with respect to salinity and turbidity values, although it applies to all measured properties except for pH. This shows the impact of both atmospheric forcing and glacial outflow, which, based on buoyant plume model theory (Kimura et al., 2014; Mankoff et al., 2016; Jenkins, 2011) and observations (Chauché et al., 2014; Osińska et al., 2021), is mainly contained in the top layer of the ocean. Therefore, the results provide information on seasonal changes in water properties and glacier–ocean interactions and can be used for the validation of previously formulated methods of GMW tracking.

The 38-month-long duration of the project allowed for the tracking of seasonal variability across all measured hydrographic properties and showed consistency in all cases (Fig. 7). Moreover, this duration permits cautious predictions regarding long-term shifts in water column properties and reveals the impact of climate change or other influential conditions in this region. Using more sophisticated techniques, it is possible to more precisely determine the nature of this variability. The quantities of chlorophyll *a*, phycoerythrin and fDOM are not presented in Fig. 6, as their measurement was significantly less frequent.

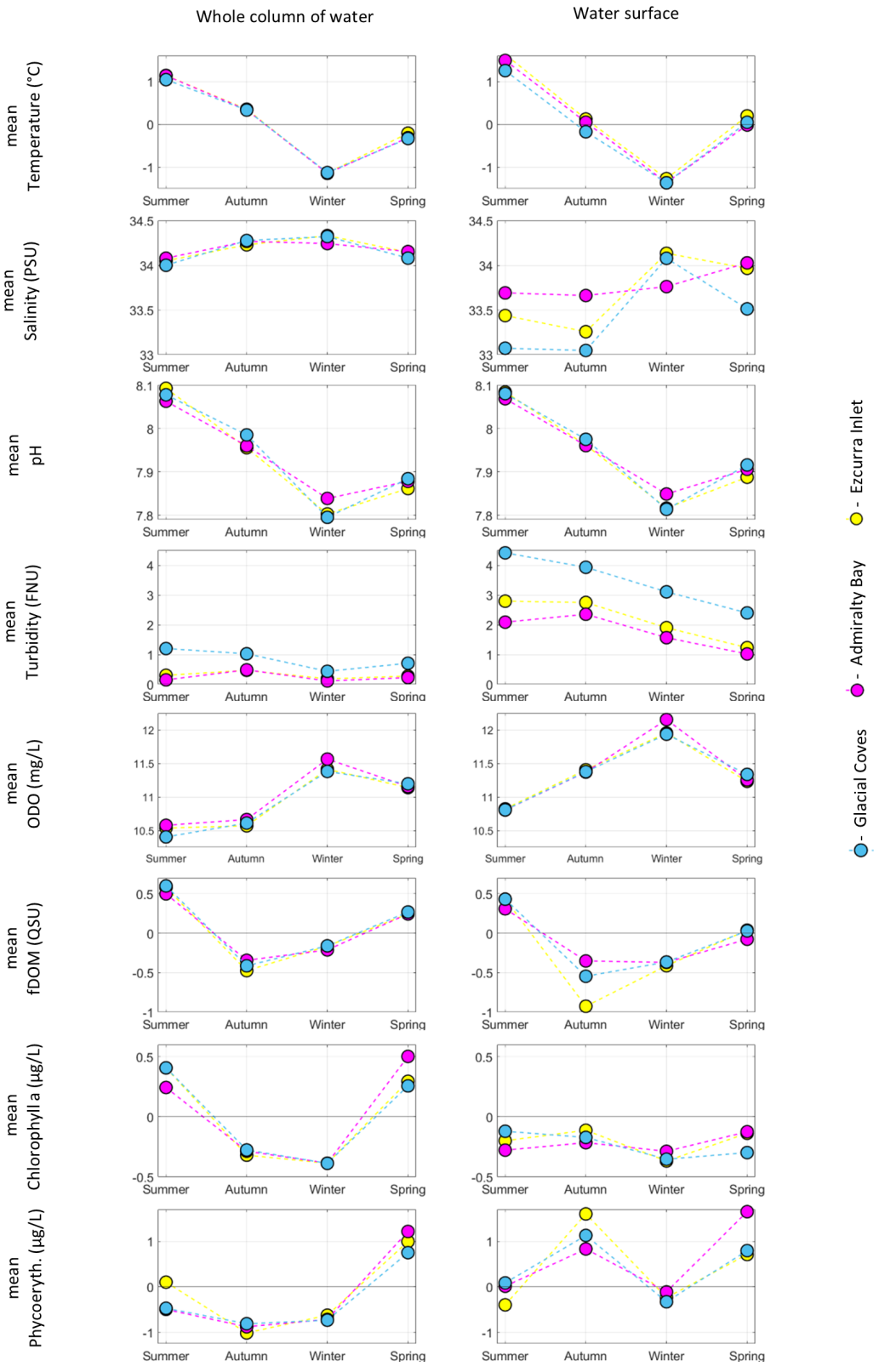

Figure 6. Mean values of measured properties dependent on season for the whole water column and the top 5 m of surface water.

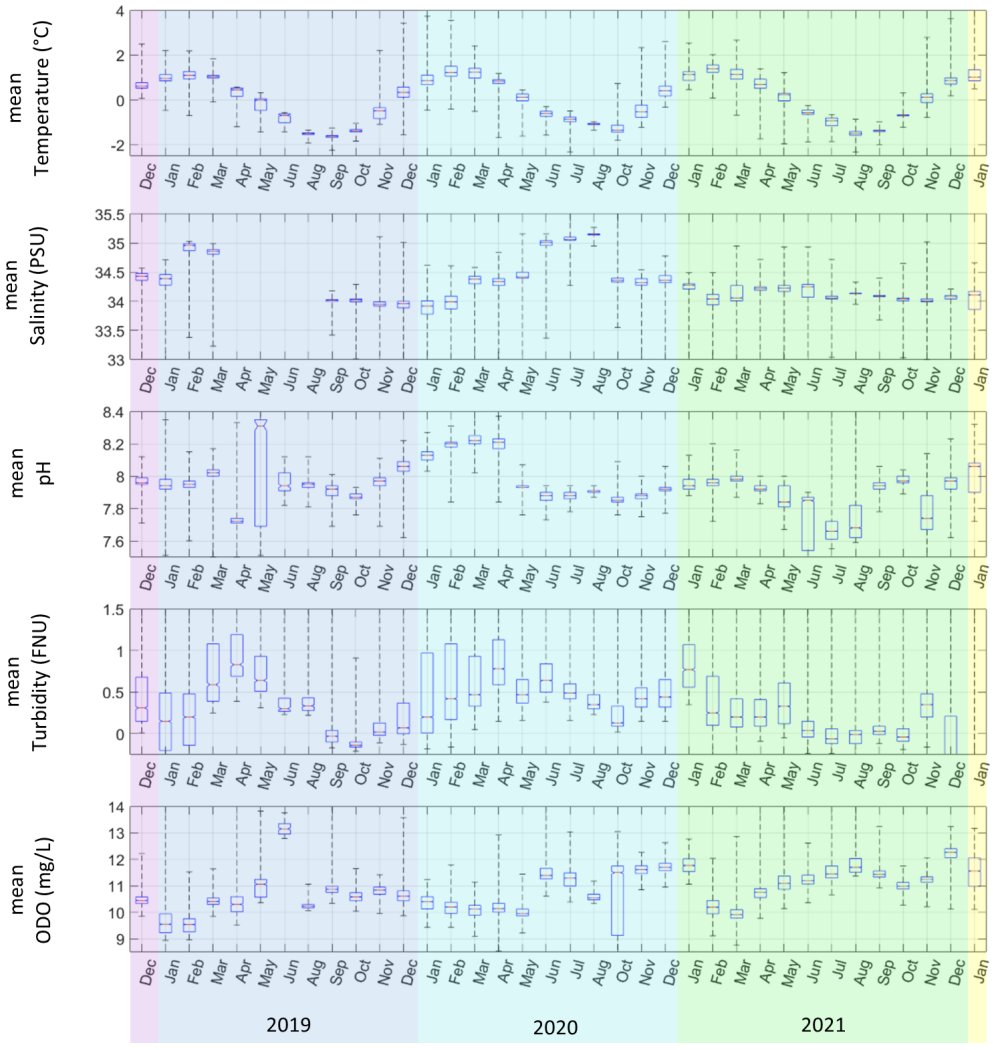

Figure 7. Box plot of monthly properties' mean values (excluding properties measured solely by EXO2 sonde devices due to their significantly shorter time series).

5 Data availability

The described dataset is freely accessible at the PANGAEA repository: https://doi.org/10.1594/PANGAEA.947909 (Osińska et al., 2022), under a non-restrictive CC BY 4.0 licence.

6 Conclusions

The assembled dataset shared here presents an opportunity to develop a better understanding of Admiralty Bay water characteristics over the 38-month survey period and can be used in further studies exploring the nature of and changes in glacially influenced regions in general. The sheer magnitude of this investigation, with 3045 separate measurements acquired on 142 different days, validates its importance and inspires optimism regarding future work and the application of these data.

The scope of the measured parameters (thermodynamic, physical, chemical and biological) paints a wide and precise picture of AB hydrographic variability during all months of the year and may allow for a multidisciplinary analysis of the complex processes that take place at this location. The varied settings of study sites allow for the tracking and identification of GMW and other water masses (Straneo et al., 2011; Chauché et al., 2014). Additionally, this sizable dataset can be used as a tool for better understanding the general hydrodynamics and thermodynamics of glacial bays and fjords and may be employed for the validation of coupled glacier–ocean modelling (Cowton et al., 2015; De Andrés et al., 2021; Bertino and Holland, 2017).

Author contributions. MO conceptualized the study; curated the data; undertook the formal analysis, investigation and validation; developed the methodology; created figures; and prepared the orig-

inal draft of the paper. KAW was responsible for carrying out the investigation, developing the methodology, and reviewing and editing the manuscript. RJB acquired funding, carried out the investigation, was responsible for project administration, acquired resources, supervised the study, and reviewed and edited the manuscript.

Competing interests. The contact author has declared that none of the authors has any competing interests.

Disclaimer. Publisher's note: Copernicus Publications remains neutral with regard to jurisdictional claims in published maps and institutional affiliations.

Acknowledgements. Calculations were made possible by software provided by CI TASK (Centrum Informatyczne TASK) in Gdańsk. The authors also wish to acknowledge the invincible members of the so-called "MorMon" team, part of Polish Antarctic Station's crew, who throughout the whole period of the project, often in trying and almost always in uncomfortable conditions, carried out the measurements presented in this work.

Financial support. This work was supported by the National Science Centre, Poland (grant no. UMO-2017/25/B/ST10/02092; Quantitative assessment of sediment transport from glaciers of South Shetland Islands on the basis of selected remote sensing methods).

Review statement. This paper was edited by Salvatore Marullo and reviewed by Mattias Cape, Luca Fiorani, and one anonymous referee.

References

APHA: Standard Methods for Examination of Water and Wastewater, 17th Edn., Washington D.C., ISBN 9780875531618, 1989.

Bendtsen, J., Mortensen, J., Lennert, K., and Rysgaard, S.: Heat sources for glacial ice melt in a west Greenland tidewater outlet glacier fjord: The role of subglacial freshwater discharge, Geophys. Res. Lett., 42, 4089–4095, https://doi.org/10.1002/2015GL063846, 2015.

Bertino, L. and Holland, M. M.: Coupled ice-ocean modeling and predictions, J. Mar. Res., 75, 839–875, https://doi.org/10.1357/002224017823524017, 2017.

Chauché, N., Hubbard, A., Gascard, J.-C., Box, J. E., Bates, R., Koppes, M., Sole, A., Christoffersen, P., and Patton, H.: Ice–ocean interaction and calving front morphology at two west Greenland tidewater outlet glaciers, The Cryosphere, 8, 1457–1468, https://doi.org/10.5194/tc-8-1457-2014, 2014.

Cowton, T., Slater, D., Sole, A., Goldberg, D., and Nienow, P.: Modeling the impact of glacial runoff on fjord circulation and submarine melt rate using a new subgrid-scale parameterization for glacial plumes, J. Geophys. Res.-Oceans, 120, 796–812, https://doi.org/10.1002/2014JC010324, 2015.

De Andrés, E., Otero, J., Navarro, F. J., and Walczowski, W.: Glacier-plume or glacier-fjord circulation models? A 2-D comparison for Hansbreen-Hansbukta system, Svalbard, J. Glaciol., 67, 797–810, https://doi.org/10.1017/jog.2021.27, 2021.

Dziembowski, M. and Bialik, R. J.: The Remotely and Directly Obtained Results of Glaciological Studies on King George Island: A Review, Remote Sens. Basel, 14, 2736, https://doi.org/10.3390/RS14122736, 2022.

Gerrish, L., Fretwell, P., and Cooper, P.: High resolution vector polylines of the Antarctic coastline (7.4), ADD – Antarctic Digital Database [data set], https://doi.org/10.5285/e46be5bc-ef8e-4fd5-967b-92863fbe2835, 2021.

Jenkins, A.: Convection-Driven Melting near the Grounding Lines of Ice Shelves and Tidewater Glaciers, J. Phys. Oceanogr., 41, 2279–2294, https://doi.org/10.1175/JPO-D-11-03.1, 2011.

Kimura, S., Holland, P. R., Jenkins, A., and Piggott, M.: The Effect of Meltwater Plumes on the Melting of a Vertical Glacier Face, J. Phys. Oceanogr., 44, 3099–3117, https://doi.org/10.1175/JPO-D-13-0219.1, 2014.

Mankoff, K. D., Straneo, F., Cenedese, C., Das, S. B., Richards, C. G., and Singh, H.: Structure and dynamics of a subglacial discharge plume in a Greenlandic fjord, J. Geophys. Res.-Oceans, 121, 8670–8688, https://doi.org/10.1002/2016JC011764, 2016.

Osińska, M., Bialik, R. J., and Wójcik-Długoborska, K. A.: Interrelation of quality parameters of surface waters in five tidewater glacier coves of King George Island, Antarctica, Sci. Total Environ., 771, 144780, https://doi.org/10.1016/j.scitotenv.2020.144780, 2021.

Osińska, M., Wójcik-Długoborska, K. A., and Bialik, R. J.: Water conductivity, salinity, temperature, turbidity, pH, fluorescent dissolved organic matter (fDOM), optical dissolved oxygen (ODO), chlorophyll a and phycoerythrin measurements in Admiralty Bay, King George Island, from Dec 2018 to Jan 2022, PANGAEA [data set], https://doi.org/10.1594/PANGAEA.947909, 2022.

Rückamp, M., Blindow, N., Suckro, S., Braun, M., and Humbert, A.: Dynamics of the ice cap on King George Island, antarctica: Field measurements and numerical simulations, Ann. Glaciol., 51, 80–90, https://doi.org/10.3189/172756410791392817, 2010.

Snazelle, T. T.: Evaluation of Xylem EXO water-quality sondes and sensors, U.S. Geological Survey Open-File Report 2015-1063, https://doi.org/10.3133/OFR20151063, 2015.

Straneo, F.: Impact of the large scale ocean circulation on Greenland's outlet glaciers, Quaternary Int., 279–280, 472, https://doi.org/10.1016/j.quaint.2012.08.1584, 2012.

Straneo, F., Curry, R. G., Sutherland, D. A., Hamilton, G. S., Cenedese, C., Våge, K., and Stearns, L. A.: Impact of fjord dynamics and glacial runoff on the circulation near Helheim Glacier, Nat. Geosci., 4, 322–327, https://doi.org/10.1038/ngeo1109, 2011.

Wójcik-Długoborska, K. A., Osińska, M., and Bialik, R. J.: The impact of glacial suspension color on the relationship between its properties and marine water spectral reflectance, IEEE J. Sel. Top. Appl., 15, 3258–3268, https://doi.org/10.1109/JSTARS.2022.3166398, 2022.

YSI Inc: Exo User Manual, Yellow Springs, 1–154 pp., 2017.